ELSEVIER

Journal of Alloys and Compounds 229 (1995) 80–92

Journal of ALLOYS AND COMPOUNDS

Multiphase reaction diffusion in transition metal–carbon and transition metal–nitrogen systems

W. Lengauer

Institute for Chemical Technology of Inorganic Materials, Vienna University of Technology, Getreidemarkt 9/161, A-1060 Vienna, Austria

Received 20 February 1995

Abstract

The suitability of using diffusion couples for the measurement of both phase equilibria and diffusivities is shown for the field of transition metal carbides and nitrides. Examples of the binary, ternary and quaternary systems Ti–N, Nb–N, Hf–N, Nb–C, Ta–C, Ti–Zr–N and TiCN–Ni are explained, together with preparation, investigation and evaluation techniques. The main topics, emphasized for binary systems in particular, are the investigation of phase equilibria by means of isothermal and temperature-gradient diffusion couples, the measurement of concentration-independent diffusivities from layer-growth data, the usefulness of wedge-shaped diffusion couples for the determination of both diffusivities and phase equilibria studies, and the evaluation of concentration-dependent diffusivities from diffusion profiles.

Keywords: Phase equilibria; Electron probe microanalysis; Second order phase transitions; Diffusion

1. Introduction

If two pure compounds having a mutual solubility and being in intimate contact with each other are annealed at an appropriately high temperature, diffusion of the components will occur as the system attempts to establish thermodynamic equilibrium, which is reached when the chemical potentials of the constituents in the phases are identical. This diffusion process occurs in a concentration (activity) gradient and is called chemical diffusion. Occasionally, one or more phases can occur between the initial phases because of a superimposed chemical reaction: a so-called reaction diffusion. It is generally accepted that thermodynamic equilibrium exists in the contact area of these grown phases. That is, such a diffusion couple exhibits an isothermal section of the system on which it is based [1]. The most information can be obtained prior to the state where overall thermodynamic equilibrium is reached and when all the phases are present in an appropriate thickness so that concentration-dependent effects can be read as a function of the distance. As will be shown, this can also be performed with the temperature axis in order to read temperature-dependent effects as a function of distance.

In many technical processes – especially where high temperatures are applied – diffusion plays a dominant role in achieving the desired state of the prepared material. This is also true for transition metal carbides and nitrides because they are high-temperature materials. They are used as coatings and in cermets for metal-shaping processes. This summary of the results obtained in our laboratory should provide some insight into how thermodynamic and kinetic data, which are difficult or even impossible to collect with other techniques, can be obtained for these materials through solid-state reaction diffusion experiments.

2. Preparation techniques

Because a good contact between a metal and the respective monocarbides and mononitrides is difficult to form, the most straightforward technique for preparing a multiphase carbide or nitride diffusion couple is to place the metals in a graphite bed or to anneal them in nitrogen atmosphere. In the case of carbide diffusion couples the carbon is transferred mainly via the gas phase by the action of impurities. Thus, even if high-purity starting materials are used, a considerable amount of carbon is transported to the metal surface.

SSDI 0925-8388(95)01683-X

The use of hydrogen, which causes the formation of hydrocarbons and thus strongly favors the transport of carbon, does not give different results, at least for the VB metal–carbon couples, but does include the danger of the formation of hydrides, and may have an undesirable influence on the diffusion process. During the diffusion process the carbide or nitride phases grow simultaneously from the outside to the inside of the sample. For some nitrides (for which the nitrogen equilibrium pressure is not too low) the nitrogen activity at the surface can be adjusted via the nitrogen pressure (at a given temperature) so that it is possible to grow a different number of phases: for example, with and without the mononitride as the outer phase. The carbon activities for the carbide diffusion couples are always unity at the surface if graphite beds are used, and subcarbides cannot be formed there.

For high-temperature heat treatments cold-wall autoclaves with tungsten heating tubes were used. The temperatures were recorded by thermocouples or two-color IR pyrometers. Gas pressures (mbar range up to 40 bar) were measured with piezoelectric gauges. The conditions were recorded on a PC equipped with an A/D converter. The design of the autoclaves is such that extended heating periods can be maintained without any change in experimental conditions.

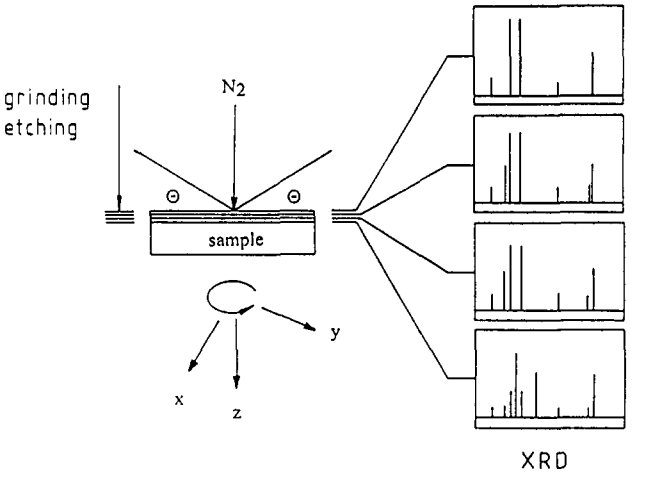

Fig. 1. Schematic representation of the investigation of a diffusion couple by Bragg–Brentano geometry in XRD phase analysis. Only the lattice planes perpendicular to the main diffusion direction can be detected because the main diffusion direction is perpendicular to the surface. The d values are the distances between these lattice planes.

3. Investigative techniques

3.1. X-ray diffraction

Phase identification was performed by X-ray diffraction in Bragg–Brentano θ–2θ geometry. For plane-sheet diffusion couples to be investigated in this geometry the detected lattice planes are perpendicular to the main diffusion direction, z, of carbon and nitrogen (Fig. 1). A rotating sample holder was preferentially applied in order to minimize texture effects in the x–y plane. Orientational effects due to diffusion generally occur relative to the main diffusion direction of the metalloid, which is the growth direction of the crystallites. A connection between growth and the diffusion direction exists since the shortest repeating distance of unit cell dimensions is in the z direction [1].

3.2. Metallography

The samples were cut perpendicular to the surface and embedded in a cold-setting resin. Then they were polished with 125 μm and 20 μm diamond discs. After ultrasonic cleaning, further polishing was carried out with 3 μm and occasionally 1 μm diamond. This procedure took about 2–5 h. For optimum phase identification in polarized light an aqueous suspension of SiO_2 was applied for polishing after diamond polishing. The SiO_2 suspension provides a combination of chemical (the pH is about 9) and mechanical attack. However, this procedure causes a surface relief on the sample, and should be avoided if the samples are to be investigated by EPMA (see Section 3.3). In some cases anodic oxidation was carried out with phosphoric or sulfuric acid.

3.3. Measurement of concentration profiles

Substantial progress in electron-probe microanalysis (EPMA) has been made in the last two decades, so that it is possible to determine ultra-light elements such as boron, carbon and nitrogen with this technique [2,3]. The lateral resolution, the high accuracy and the high degree of automation for performing line-scans make EPMA a unique tool for the determination of diffusion profiles as long as the thickness of the layer is greater than 10 μm.

In the present study a Cameca SX50 microprobe was used, which initially was equipped with four, and in later studies five, spectrometers and a variety of crystals ranging from W/Si multilayer crystals with a lattice spacing of 100 and 60 Å respectively to crystals for heavy elements. The W/Si crystals have a poorer resolution but a much better peak-to-background ratio and a better background function than non-artificial crystals such as lead stearate. The microprobe scans were usually applied in the step scan mode with a counting time of 6–30 s per step, 60–300 nA beam current and 10–15 kV voltage. The PAP model [4] for the description of the mass–depth curve was used in

the concentration calculations. Throughout the EPMA analyses homotypic standardization was applied [5], meaning that homogeneous single-phase samples from the system under investigation were used as standards. These standards were chemically analyzed. This procedure should provide a better calibration because carbon and nitrogen line shifts due to the influence of chemical bonding and any unusual background shapes could be better corrected. The longer counting time and the higher beam current were applied for diffusion couples that contained very heavy elements such as Ta. In the course of the most recent optimizations for this technique a liquid-nitrogen cold trap and an oxygen jet were applied in order to avoid any drift in the carbon scans due to enrichment of hydrocarbons stemming from the gas phase, from resin around the samples and from the metallographic preparations. The oxygen inlet was set so that the pressure in the sample chamber reached 3×10^{-4} mbar.

Precautions had to be taken to keep the sample as flat as possible during the metallographic preparation process. Light-optical microscopy requires a high-quality preparation if the often very small differences in appearance between different phases are to be properly distinguished. As mentioned above, this was possible when an aqueous silica suspension was used in the very last polishing step. A major disadvantage of this preparation technique, however, is the pronounced surface relief that it causes, which can be unfavorable for EPMA investigation, where a flat specimen with small differences in height between crystallites is best. These opposing requirements are further complicated by the fact that the relief-polished surface also helps in locating the appropriate places in the microprobe, which is normally equipped with a microscope of poorer quality than metallographic microscopes.

A rapid check for the presence of surface relief effects can be made by plotting the total amount of constituents vs. distance. For this procedure it is necessary to measure all constituents. The influence of surface reliefs can be seen from Fig. 2 for a Ta–C couple, where this effect is very pronounced because of the low amount of carbon. The carbon profile (top) in the inner β-Ta_2C phase is obviously not symmetric. A corresponding discontinuity can be observed in the analytical total (bottom) which shows the left part below 100% and the right part above 100%, indicating a difference in the detected total radiation relative to that of the standardizing procedure. This difference stems from the variations in crystallite height caused by polishing. In heavily relief-polished samples, discontinuities at both interphase as well as intraphase boundaries could be observed because of different heights due to different hardnesses.

Relief effects in diffusion couples have not yet been

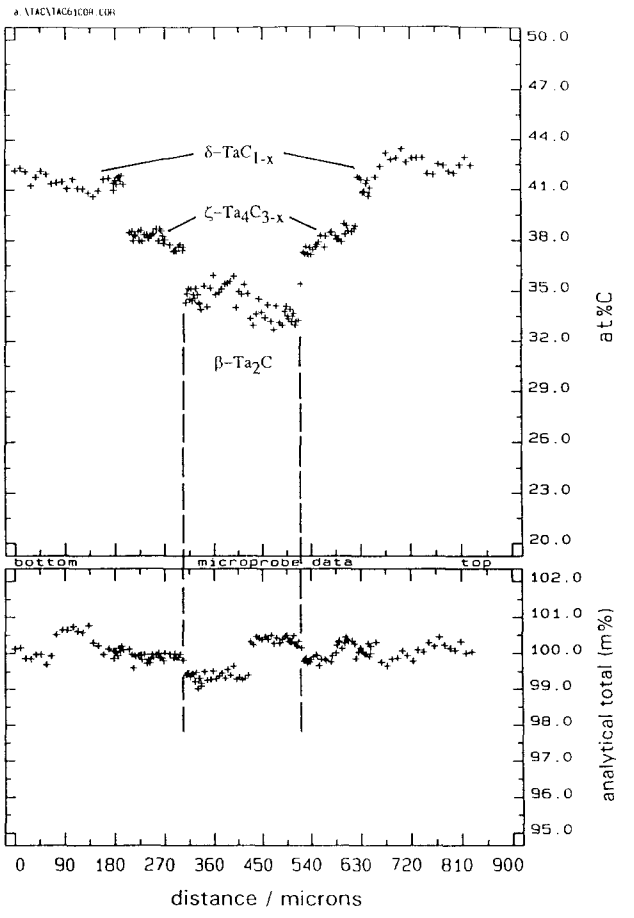

Fig. 2. EPMA results from a Ta–C diffusion couple. Top: carbon concentration profile. Bottom: analytical total (sum of carbon and tantalum analysis). The jump of the measured analytical total in the β-Ta_2C core phase is due to a relief effect.

reported in the literature. However, when Bastin *et al.* [6] measured the nitrogen concentration profile of a nitrided titanium sample, they measured the edges of a TiN couple twice, turning it after the first scan. With this procedure they found a difference between the results of the two scans, showing the round-off of the sample edge upon polishing. In both cases a nitrogen content well below 50 at.% N was found, and hence they concluded that the surface was substoichiometric. However, it can be proven experimentally (XRD) that TiN has a strictly stoichiometric composition not only at the applied conditions but even at nitrogen pressures several orders of magnitude lower. Therefore the apparent substoichiometry can only be explained by the facts that the outermost few μm are practically inaccessible by standard metallography, together with the fact that the nitrogen profile is very steep at these depths because of a concentration-dependent diffusivity. A measurement from our laboratory shows this steepness in the profile (Fig. 3).

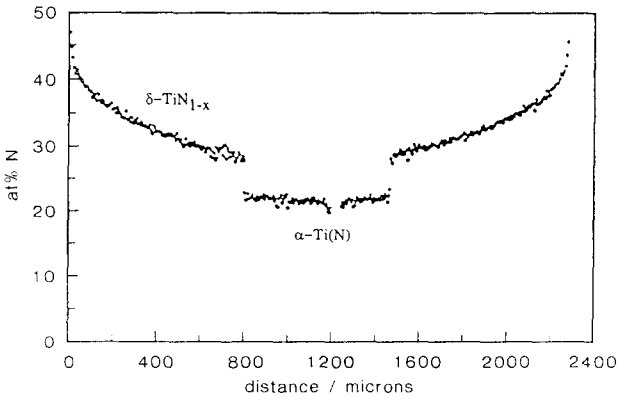

Fig. 3. Nitrogen profile in a plane-sheet Ti–N diffusion couple annealed at 1600 °C for 7.5 h in nitrogen (3 bar). A steep concentration profile forms near the surface, which does not allow one to measure the surface concentration by EPMA together with normal cross-sectional metallographic preparation. However, it can be proven (e.g. XRD) that the surface concentration of δ-TiN_{1-x} is indeed 50 at.% N.

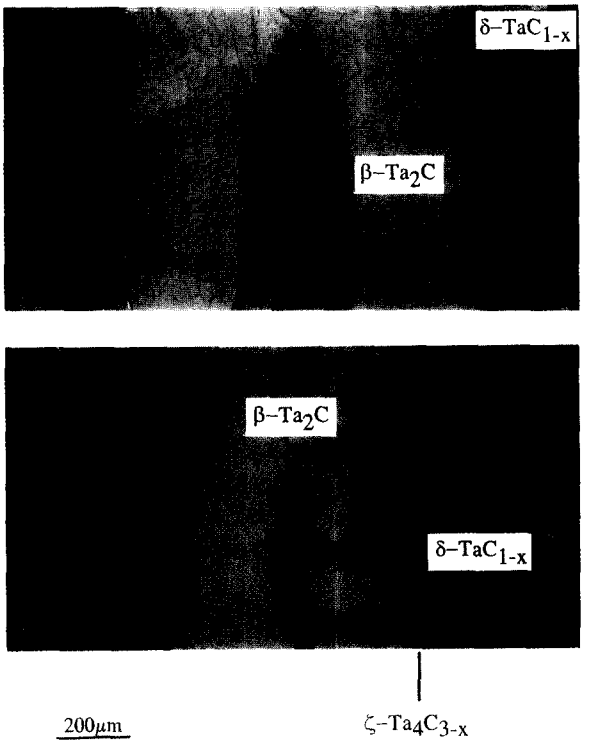

Fig. 4. Microstructures of wedge-shaped Ta–C diffusion couples (anodically oxidized with phosphoric acid; polarized light). Top: annealed at 2175 °C; the ζ-Ta_4C_{3-x} phase is absent between β-Ta_2C and δ-TaC_{1-x}. Bottom: annealed at 2147 °C; the ζ-Ta_4C_{3-x} phase is present. These results are indicative of a invariant phase reaction β-$Ta_2C + \delta$-$TaC_{1-x} \rightarrow \zeta$-$Ta_4C_{3-x}$ at 2147–2175 °C [8].

4. Results and discussion

4.1. Invariant temperatures determined with diffusion couples

4.1.1. Isothermal diffusion couples

Probably the best-known characteristic of reaction diffusion couples is their unique suitability for establishing portions of phase diagrams. Diffusion couples, annealed at different temperatures, give a picture of phase reactions at these temperatures, so that it is often possible to determine the formation or decomposition temperature of a phase. Such a result is shown in Fig. 4 for the ζ-Ta_4C_{3-x} phase [7]. At $T \geq 2175$ °C the layer sequence is δ-TaC_{1-x}/β-Ta_2C/α-Ta(C) and at $T \leq 2147$ °C the layer sequence is δ-TaC_{1-x}/ζ-Ta_4C_{3-x}/β-Ta_2C/α-Ta(C). In other words, the ζ-Ta_4C_{3-x} phase decomposes between these two temperatures. Upon measurement of the carbon diffusion profiles, isothermal sections of the Ta–C system could be determined. This information helped us to establish a more precise phase diagram [8]. If narrow diffusion bands such as that for ζ-Ta_4C_{3-x} are observed, EPMA is preferentially carried out on samples of restricted sample geometry. This enhances the thickness of diffusion layers (see Section 4.3).

4.1.2. Temperature-gradient diffusion couples

A further step in the determination of decomposition/formation temperatures of phases is possible if a temperature gradient is introduced in a diffusion couple in such a way that it is perpendicular to the concentration axis. The axes are then in the same configuration as that used for the usual representation of a phase diagram, T vs. composition. The temperature gradient causes an additional nitrogen flux (Soret effect [9]), which can be parallel or anti-parallel to the gradient, depending on the sign of the transport energy Q. For metalloid diffusion in transition metal carbides and nitrides $Q < 0$ so that the flux is from the cool end of the temperature interval to the hot end. Thus the phase boundaries move slightly (but hardly detectable within the applied conditions). It can be concluded that the additional flux does not perceptibly influence the equilibrium conditions between the phase bands in any direction, analogous to the situation for the isothermal case where thermodynamic equilibrium (or a state very near to it) also exists locally at slow-moving interfaces.

This temperature-gradient diffusion couple technique was developed for temperatures where the samples could be placed in silica tubes for protection against the ambient atmosphere, and was applied for diffusion couples of the Ti–N system, where several invariant reactions occur in a small temperature interval [10], which is not accessible for individual isothermal experiments. The temperature intervals had to be carefully chosen under consideration of isothermal

results because the diffusivity is strongly temperature-dependent. Thus the layers would be much thicker at the high-temperature end than at the low-temperature end of the couple. The experiment was therefore performed in such a way as to re-anneal an already isothermally prepared couple (prepared at an intermediate temperature) in the gradient in order to anticipate the largest amount of the diffusion process within the isothermal part (e.g. formation of the thick δ-TiN_{1-x} layer). The temperature-gradient annealing was then carried out for a relatively short time since only short nitrogen diffusion distances had to be overcome to stabilize a sequence of thin subnitride layers. The short reheating cycle also provides good temperature stability of the heating device.

The grain boundary structure of a temperature-gradient diffusion couple is shown in Fig. 5 (the true microstructures are readily visible only in a high-quality color reproduction [10]). These figures were obtained by tracing the grain boundaries of the TGDC microstructures. Whenever the phase band sequence changes (appearance or disappearance of a phase band) a non-variant phase reaction takes place. Fig. 5, left part, illustrates the formation of η-Ti_3N_{2-x} from α-Ti(N) and ε-Ti_2N at 1066 °C. Fig. 5, right, contains the traced microstructure of two non-variant phase reactions: η-Ti_3N_{2-x} + ε-$Ti_2N \rightarrow \zeta$-Ti_4N_{3-x}, at 1078 °C, and ε-$Ti_2N \rightarrow \zeta$-Ti_4N_{3-x} + δ-TiN_{1-x}, at 1080 °C.

It is clear that such phase reactions cannot be determined by DTA [11] and/or quenching experiments. Thus it would be desirable to design similar experiments for higher temperatures, where silica tubes cannot be applied and instead high-temperature furnaces are used. A variety of questionably invariant temperatures can be found in the literature [8], not only in carbide and nitride systems.

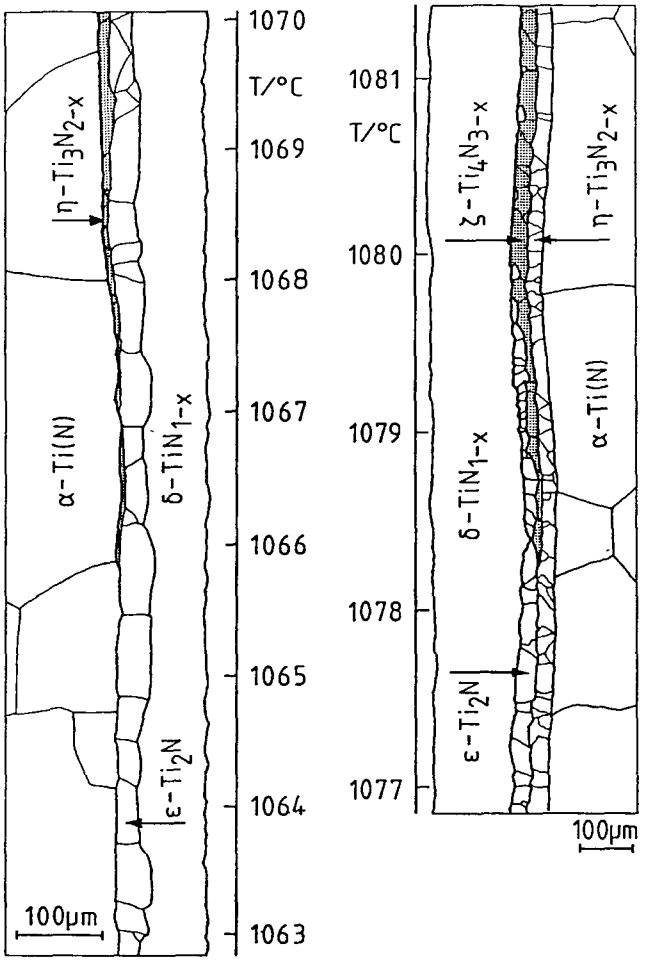

Fig. 5. Temperature-gradient diffusion couples, which resolve the phase reactions in a narrow concentration and temperature interval of the Ti–N system. Left: formation of η-Ti_3N_{2-x} at 1066 °C (invariant reaction ε-Ti_2N + α-Ti(N) $\rightarrow \eta$-Ti_3N_{2-x}). Right: formation of ζ-Ti_4N_{3-x} at ≈1078 °C and decomposition of ε-Ti_2N at 1080 °C (phase reactions η-Ti_3N_{2-x} + ε-$Ti_2N \rightarrow \zeta$-Ti_4N_{3-x} and ε-$Ti_2N \rightarrow \zeta$-Ti_4N_{3-x} + δ-TiN_{1-x}, respectively).

4.2. Diffusivities obtained from layer growth data

The layer growth in multiphase diffusion couples has been treated by several authors, e.g. Wagner cited in [12], and Kidson [13]. The diffusion problem within carburization and nitridation where a carbide or nitride surface layer is formed is graphically represented in Fig. 6 for three phases, where ξ_i are the positions of

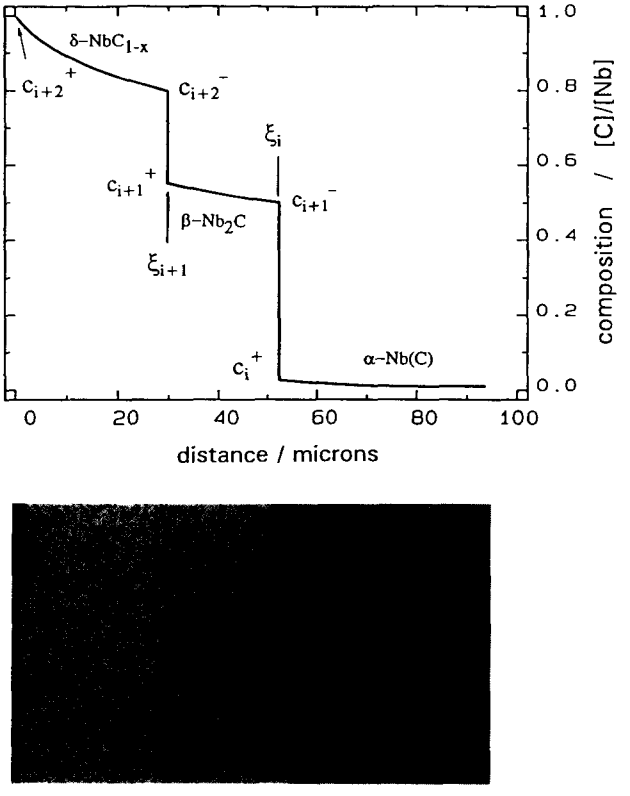

Fig. 6. Top: schematic diffusion profile in a three-phase diffusion couple. Bottom: corresponding microstructure, Nb–C couple; phase 3, δ-NbC_{1-x}; phase 2, β-Nb_2C; phase 1, α-Nb(C).

the interfaces between the phases. The growth of a diffusion layer at constant temperature is given by

$$\xi_i = 2k_i(D_i, D_{i+1}, \Delta c_i, \Delta c_{i+1})\sqrt{t} \quad (1)$$

where ξ_i is the layer thickness of phase i; D_i, D_{i+1} are the diffusivities of carbon or nitrogen in the phase i and $i+1$ respectively; Δc_i, Δc_{i+1} are the homogeneity ranges of phases i and $i+1$ respectively; t is the diffusion time; and k_i is a known function of the values given in parentheses. The function k_i (for an analytical expression see [14]) does not depend on the diffusion time if the process is diffusion controlled (that is, when the layers grow simultaneously and no reaction-controlled mechanisms exist) and if the geometry is semi-infinite. Eq. (1) states the parabolic law of layer growth (Tammann's rule).

The movement of an interface between two diffusion bands of phases i and $i+1$, $\mathrm{d}\xi_i/\mathrm{d}t$, in a multiphase binary system is proportional to the surplus of substance that arrives at the interface (which for a two-phase system is equal to ξ_i) over that which leaves the interface and enters phase 1:

$$\Delta c \frac{\mathrm{d}\xi_i}{\mathrm{d}t} = J_i - J_{i+1} \quad (2)$$

where J_i and J_{i+1} are the fluxes of material leaving and arriving at the interface respectively, and Δc is the difference in composition of the two phases at the interface. After Fick's first law, Eq. (2) can be given as

$$\Delta c \frac{\mathrm{d}\xi_i}{\mathrm{d}t} = D_i \left.\frac{\partial c}{\partial x}\right|_i - D_{i+1} \left.\frac{\partial c}{\partial x}\right|_{i+1} \quad (2a)$$

where D_i and D_{i+1} are the diffusion coefficients of the metalloid in the two phases respectively, and $(\partial c/\partial x)_i$ and $(\partial c/\partial x)_{i+1}$ are the derivatives of the concentrations on either side of the interface respectively.

A possible solution of Eq. (2a) is to assume an error function for the concentration profiles in the two phases and to insert that into Eq. (2). The reader is referred to standard textbooks for this procedure (e.g. [15], p. 25). From this equation it is then possible to determine the thicknesses of phase bands by knowing the diffusivities in the respective phases. However, as already stated by Jost [12] as well by Philibert [15], the thickness measurements of diffusion layers in a series of diffusion experiments annealed at a given temperature for a number of different durations cannot give the absolute values of the diffusion coefficients if not a single diffusivity is known or neglected (e.g. for zero solubility of a component in the metal) because there are two unknown coefficients D_i, D_{i+1} but only one equation, Eq. (1) or Eq. (2a). In some cases with the application of finite diffusion geometry a solution to that problem is possible that allows one to measure all the diffusivities. This is shown in Section 4.3.

4.3. Influence of restricted diffusion geometry on layer thickness

According to the relationship above the diffusion-controlled growth of phase bands is parabolic (Eq. (1)). This is true only for the case of semi-infinite diffusion geometry. In the case of restricted geometry the phase bands grow faster than in the semi-infinite case, which means that the growth parameter k increases at a given time as the size of the sample decreases – or vice versa – with time at a given thickness. Restricted diffusion geometry has been described by Crank [16], but for multiphase diffusion nothing has been reported since the work by Pawel and Campbell [17] on the oxidation of sheets of Zr alloys.

For plane-sheet geometry the influence of restricted diffusion geometry on the development of phase bands can be shown in a quite straightforward way by using wedge-type diffusion couples, provided that the wedge angle is small so that to a good approximation it represents plane-sheet diffusion behavior. Numerous samples with different thicknesses are represented by such a wedge-type sample, all of which can be annealed and investigated at the same time. Such a diffusion couple is shown in Fig. 7 for the Hf-N system [18]. It can be seen that the ζ phase band increases as the thickness of the sample decreases. This is caused by an increasing exhaustion of the sink (saturation of the respective core phase) upon decreasing sample thickness. Because of this the diffusion profile flattens, which in turn causes the phase bands to expand owing to the thermodynamic constraint of fixed boundary concentrations. This phase-band expansion can be used to determine the presence or absence of otherwise thin diffusion bands (phase stability, compare Section 4.1.1.) and to measure the homogeneity regions of otherwise narrow bands even using laterally restricted microanalytical techniques such as EPMA (lateral resolution about 2 μm). This is especially valuable if light elements have to be determined in the

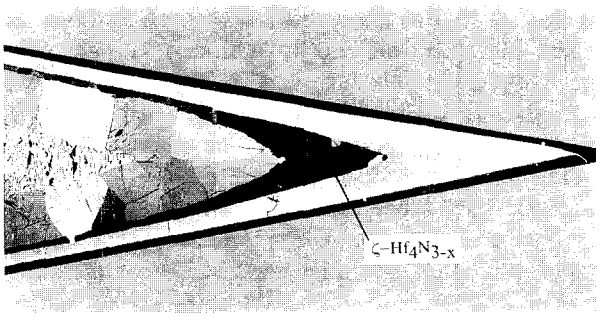

Fig. 7. Wedge-type sample of the Hf–N system prepared by annealing Hf metal in nitrogen atmosphere (71 h, 1650 °C, 10 bar N_2). Note the increase of the phase band thickness of the ζ-Hf_4N_{3-x} phase with decreasing sample thickness.

presence of heavy elements, since the inaccuracy due to data scatter can be overcome by placing many more point measurements along a phase band. Thus not only the average concentration but also the homogeneity range can be determined [18].

In the Hf–N system a very large thickness enhancement was found [19] so that it was possible to prepare single-phase hafnium subnitrides by performing diffusion couple experiments in which the desired phase was in the center of the couple to create a large core, followed by subsequent removal of the outer layer(s) by grinding and/or cutting. With this technique the ζ-Hf_4N_{3-x} phase could be prepared in single-phase form [19], which is not possible by standard methods such as arc-melting or hot-pressing.

An additional interesting point in the usefulness of wedge-shaped diffusion couples (quasi plane-sheet) or an array of plane-sheet diffusion couples of different thicknesses is the possibility of measuring the metalloid diffusivities in *all* the phases present, provided that a thickness enhancement can indeed be observed (otherwise the sample behaves as if it were semi-infinite). As follows from the formalism given in Section 4.2, in semi-infinite samples only the ratios of diffusivities (D_1/D_2) can be obtained from a series of thickness measurements on diffusion layers, because k_i does not depend on the diffusion time. On the other hand, for a plane-sheet couple this set of equations changes to the form

$$\xi_i = 2k_i(D_i, D_{i+1}, \Delta c_i, \Delta c_{i+1}, t)\sqrt{t} \qquad (1a)$$

where k_i is a known function with a time dependence (an analytical expression for k_i is given in [14]). Thus for the application of at least two different diffusion times, two different equations (1a) for two variables D_i and D_{i+1} exist and thus can yield the absolute values of all the diffusivities in all the phases in the diffusion couple. Because of the reciprocal relationship of space and time, expressed in the Boltzmann variable $y = x/2\sqrt{t}$, two different thicknesses for a given time also yield all the diffusivities.

The experimental verification is preferentially performed by measuring the layer thicknesses in wedge-type samples at more than two sites with different thicknesses or by preparing more than two plane-sheet diffusion couples with different thicknesses since then a good average value of each of the D_is can be obtained. This procedure has a further advantage in that only a single experiment is necessary for a given temperature, thus avoiding the large error introduced by even slightly different temperatures of multiple diffusion experiments. In our laboratory, D. Rafaja has designed computer programs to implement these formalisms and evaluate diffusivities [20]. As a result of the investigation of wedge-shaped and plane-sheet diffusion couples the concentration-independent diffusivities of metalloids in a variety of carbide and nitride phases have been measured [8,18] after the homogeneity regions of these phases were reinvestigated. Examples of the nitrogen diffusivities in hafnium nitride phases are shown in Fig. 8, from which it can be seen that the activation energy of nitrogen diffusion is independent of the nitrogen content since the transport mechanism in these phases is the same (diffusion via octahedral sites).

Multiphase diffusion in spatially restricted areas or – because of $y = x/2\sqrt{t}$ – relatively long diffusion periods are important in technical applications. The geometry can be plane parallel, as in the oxidation or dip coating of sheets, or cylindrical, as in the fiber–matrix interaction or the preparation of Nb_3Sn superconducting multi-filaments, or (nearly) spherical, as for powder particles in P/M parts. In view of its technical importance it is surprising that this phenomenon has as yet attracted so little attention, an exception being the oxidation of Zr alloy sheets in fission reactor safety design [17].

4.4. Concentration-dependent diffusivities

The monocarbides and nitrides in the rock-salt structure have a large region of homogeneity; in other words, the vacancy concentration varies from near zero to sometimes more than 50% (as in δ-TiN_{1-x} at high temperatures). It is therefore not surprising that the diffusivity is strongly concentration dependent. This dependency has not been studied in detail by chemical diffusion couples since the work published by

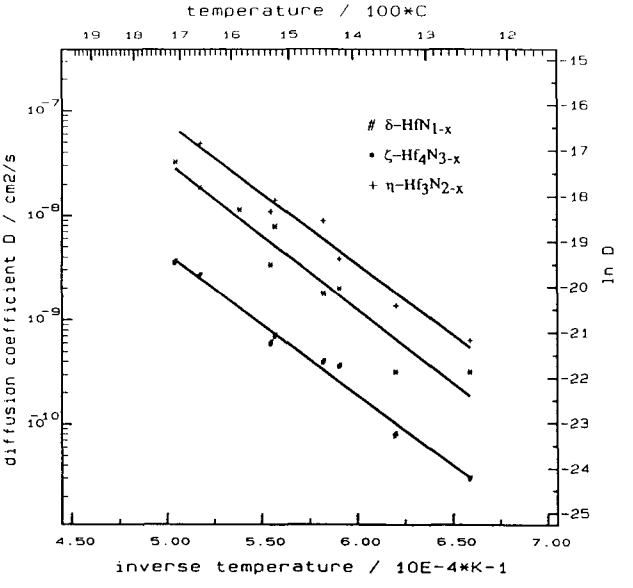

Fig. 8. Arrhenius plots of the nitrogen diffusivities in the various hafnium nitride phases. The activation energy (slope) is identical (2.75 eV), representative of an identical diffusion mechanism.

van Loo *et al.* [21] for TiC and ZrC. A study in our laboratory is in progress [22] with the aim of measuring this dependency in a variety of f.c.c. carbides and nitrides. It is based on the analytical solution of the diffusion equations with a concentration-dependent diffusion coefficient. The concentration profile is calculated in an iterative procedure until satisfactory agreement (expressed in a reliability value) is reached with the EPMA data obtained on multiphase diffusion couples of the type shown in Fig. 6. In these calculations it is assumed that the diffusion coefficient is exponentially dependent on the concentration:

$$D(c) = D_0 \exp(-Q/kT) \exp[-\alpha(c_{max} - C)] \quad (3)$$

where $D(c)$ is the concentration-dependent diffusion coefficient, $D_0 \exp(-Q/kT)$ has the usual meaning, c is the concentration of carbon or nitrogen, given respectively in mole carbon or nitrogen per cm^3 of the compound, c_{max} is the maximum nonmetal concentration in the investigated composition range (metalloid-rich boundary) and α is a constant.

Initial results of this evaluation are shown in Figs. 9 and 10 for an Nb–C couple. Fig. 9 shows the carbon diffusion profile as determined by EPMA and recalculated using unit cell volumes to give the concentration in mole carbon per cm^3 of compound. The latter was used to calculate the concentration dependence of the carbon diffusivity in δ-NbC_{1-x} for the temperature range 1500–2100 °C, which yielded the following (compare Eq. (3)):

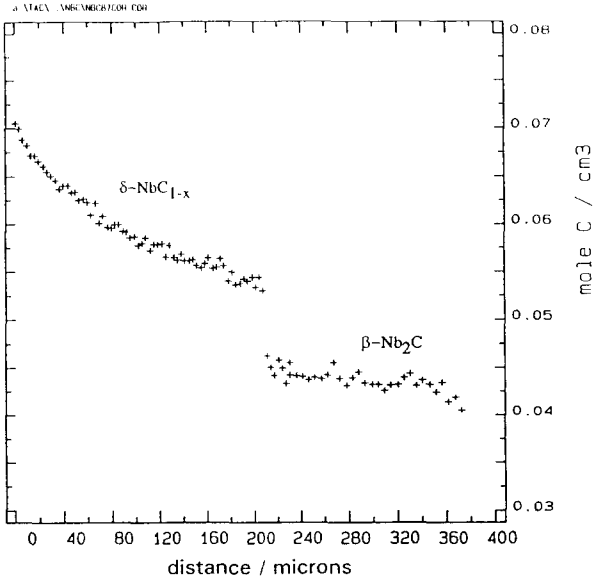

Fig. 9. Carbon diffusion profile in a Nb–C diffusion couple annealed for 23 h at 1896 °C. Recalculated profile from an EPMA measurement used for the evaluation of the concentration-dependent carbon diffusivity in δ-NbC_{1-x}.

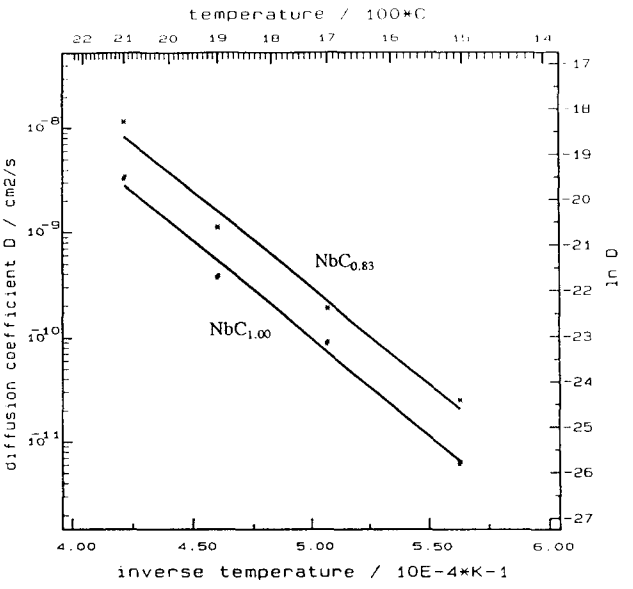

Fig. 10. Arrhenius dependencies of the carbon diffusion coefficients at the highest and lowest concentrations in δ-NbC_{1-x} as obtained from carbon profiles as shown in Fig. 9. The activation energy is independent of the concentration.

$D_0 = 0.47\ cm^2\ s^{-1}$

$Q = 3.68$ eV

$\alpha = 110.4\ mol^{-1}\ cm^3$

$c_{max} = 0.0723\ mol\ cm^{-3}$

Fig. 10 gives an Arrhenius plot for the highest and lowest concentrations of δ-NbC_{1-x} where the constancy of the activation energy (which is represented by the slope) of the carbon diffusion process can be seen. This is the same result as for the hafnium nitride phases, where the diffusion mechanism is identical for all compositions and the variation in diffusivity is reflected by a change in the frequency factor D_0.

4.5. Observations of concentration-dependent martensitic transformations

Some transformations in transition metal nitride systems cannot be suppressed by quenching, which is an indication that they are not diffusion-controlled but are instead martensitic transformations. These transformations can occur only in a certain concentration range of a compound and temperature range. Two examples are the formation of various metastable phases in the vanadium–nitrogen system [8] and the δ-$NbN_{1-x} \rightarrow \gamma$-$Nb_4N_{3-x}$ transformation upon cooling.

Wedge-type samples were prepared of the latter system, which show the transformation in the microstructure. From this the concentration dependency can be immediately seen (Fig. 11, top), since the curve of the boundary where the martensitic phase precipi-

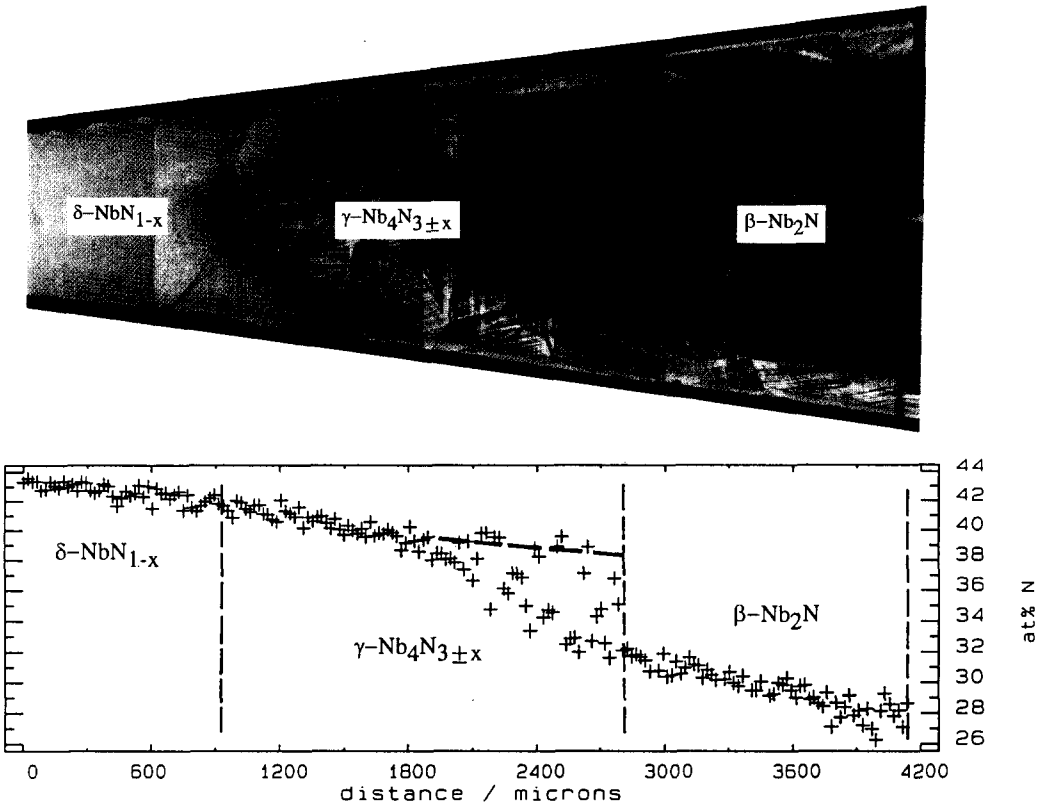

Fig. 11. Top: martensitic transformation δ-$NbN_{1-x} \rightarrow \gamma$-$Nb_4N_{3-x}$ observed in a wedge-shaped diffusion couple annealed at 1777 °C for 2 h at 30.5 bar N_2. Bottom: the line scan shows that the transformation occurs in the δ-NbN_{1-x} phase at 38.9–41.7 at.% N. The outermost part does not transform. The surface concentration of this sample is $NbN_{0.79}$ (44 at.% N).

tation occurs has the same shape as an interphase boundary. The measurement of the concentration range where this transformation occurs is possible by EPMA, as shown in Fig. 11, bottom. It can be seen that a concentration jump between δ-NbN_{1-x} and γ-Nb_4N_{3-x} is absent because no two-phase region exists. The determination of the nitrogen-poor concentration of γ-Nb_4N_{3-x} is somewhat difficult because of the scatter due to β-Nb_2N precipitations (which could be suppressed by more rapid quenching). Taking the highest EPMA values in the γ/β area (which are supposed to be free from an influence of β-Nb_2N) a linear regression gives 38.9–41.7 at.% N for the composition of the γ-Nb_4N_{3-x} region for $T = 1777$ °C. Further investigations have to be performed in order to show whether a two-phase field between γ-Nb_4N_{3-x} and δ-NbN_{1-x} exists at low temperatures [23].

4.6. Orientational effects in layer growth

The orientational effect occurring during layer growth is reflected in an X-ray diffractogram of an ε-Ti_2N layer, and becomes apparent when the experimental and calculated diffractograms are compared (Fig. 12). It can be seen that essentially only a single very strong (002) diffraction line actually occurs (top) as compared with the calculated powder diffractogram (bottom). This result shows that the unit cell of ε-Ti_2N (anti-rutile type, tetragonal structure, $a =$ 0.483 88 nm, $c = 0.303\,66$ nm) is indeed oriented in such a way that the shortest repeating distance is in the direction of nitrogen diffusion (c axis parallel to this direction), as was found for a variety of interstitial compounds by van Loo and co-workers [24].

The dependency of orientation on the main diffusion direction can also be seen in a microstructure from Fig. 13. When investigated in polarized light the color of the ε-phase band changes at a corner owing to the different orientation relative to the polarizator.

4.7. Reaction diffusion in ternary and quaternary nitrides and carbonitrides

4.7.1. The system Ti–Zr–N

According to the Gibbs phase rule in higher-than-binary systems there are one (ternary systems) or more (quaternary and higher-order systems) additional degrees of freedom, making complicated diffusion paths possible. These can be determined when the average total composition is plotted onto a concentration diagram (i.e. on a Gibbs triangle in the case of a ternary system). Formation of an intermediate phase need not necessarily occur if the boundary phases are

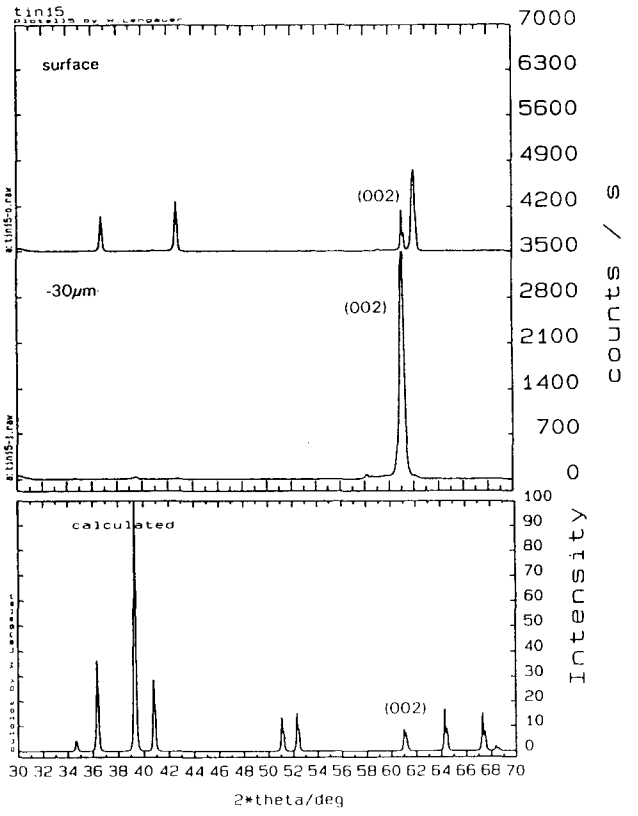

Fig. 12. XRD patterns of a Ti–N diffusion couple taken in the geometry given in Fig. 1 at the surface (top) and after removal of 30 μm (center). The top figure shows the XRD pattern of f.c.c. δ-TiN_{1-x}; the middle figure shows the XRD pattern of the ε-Ti_2N diffusion band. Essentially only one strong reflection (002) is observed for ε-Ti_2N, which is indicative that the c axis of the tetragonal unit cell is perpendicular to the surface and parallel to the main diffusion direction. Bottom: calculated powder pattern of ε-Ti_2N.

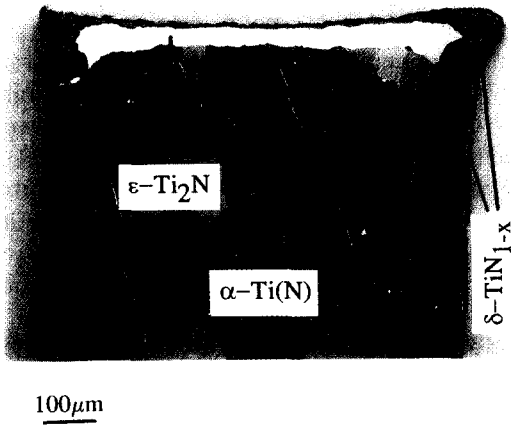

Fig. 13. Microstructure of an ε-Ti_2N phase band, which shows the orientational relationship relative to the surface. The main diffusion direction of nitrogen is perpendicular to the surface.

contacted, since the diffusion path could be of such a form that it does not pass the phase [1].

The nitridation of Ti/Zr alloys was recently investigated in order to observe the phase formation in a ternary system. TiN and ZrN have useful properties, so a modification by partial replacement of Ti through Zr could be expected to bring some new non-additive behavior. The phase reactions in this particular ternary system were of special interest since the systems of Ti–N and Zr–N are quite dissimilar with respect to the numbers of phases [23]. Furthermore, it was a good opportunity to determine how TiZrN can be prepared through the nitridation route, taking into consideration the possibilities of various diffusion paths.

A major result of these nitridation experiments was a dramatic shift in the Ti/Zr ratio for Ti/Zr alloys with a starting composition other than Ti/Zr = 60/40 at.%. In alloys with a Ti content higher than 60 at.%, Zr was enriched in the core of the sample, while in alloys with a lower Ti content Ti was enriched. Only the 60/40 alloys showed a constant Ti/Zr profile (Fig. 14). This behavior can be attributed to a diffusion path that deviates from the connecting line

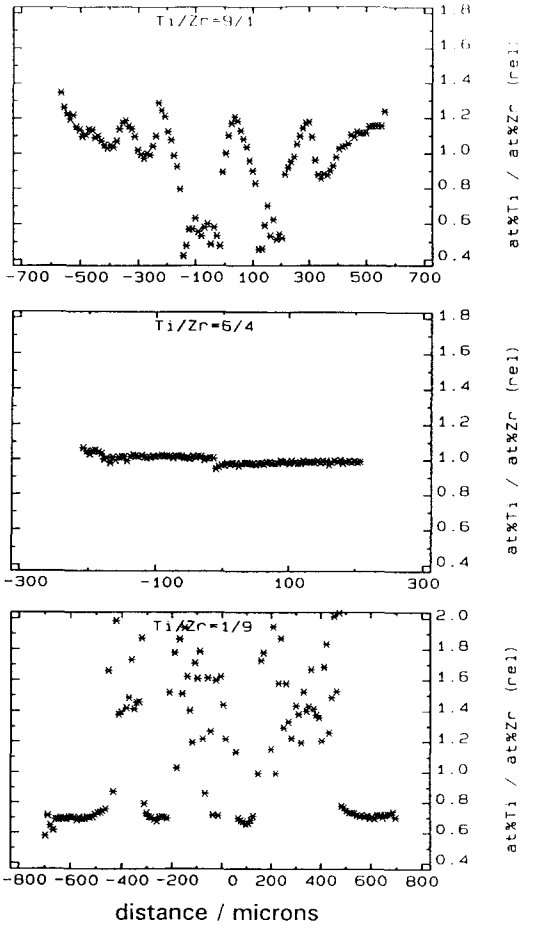

Fig. 14. EPMA of Ti–Zr–N diffusion couples annealed for 14 h at 1300 °C. Starting molar ratios Ti/Zr before nitridation: top, Ti/Zr = 9/1; center, Ti/Zr = 6/4; bottom, Ti/Zr = 1/9. The metals are inhomogeneously distributed upon nitridation except at Ti/Zr = 6/4.

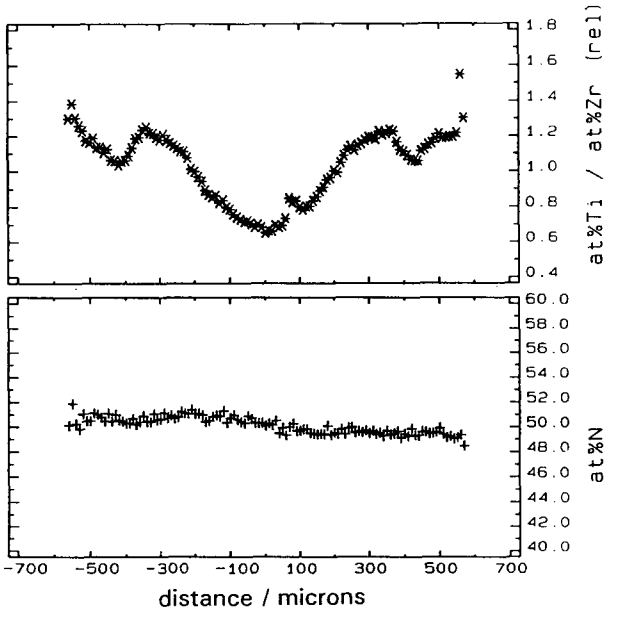

Fig. 15. Completely nitrided Ti/Zr = 90/10 alloy (annealed for 350 h at 1600 °C in nitrogen), which shows a large variation in the Ti/Zr ratio in the cross-section.

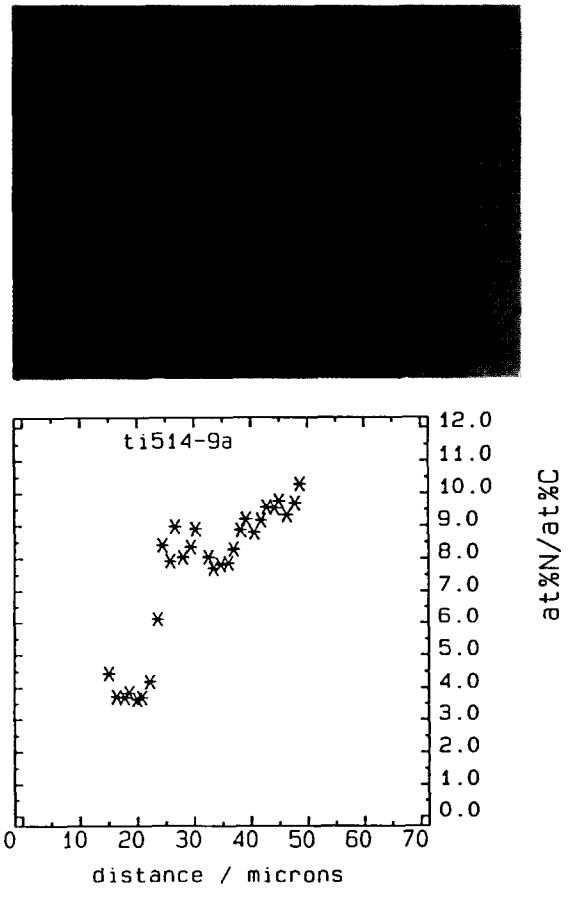

Fig. 16. EPMA in a $TiC_{0.2}N_{0.8}$ reacted at 1500 °C for 20 min with liquid nickel in a contact reaction couple. TiC is preferentially dissolved from the outer rim [26].

alloy composition–nitrogen for alloys with other than 60 at.% Ti. For this reason it is not possible by the nitridation route to obtain homogeneous Ti/Zr alloys (except 60 at.% Ti alloys), which would be required to measure solid-state properties (Fig. 15).

4.7.2. Contact reaction TiCN–liquid Ni

This type of reaction is very interesting for the liquid-phase sintering of titanium-based hardmetals (sometimes called cermets). In cermets the interaction of liquid nickel with phases like TiMoCN causes a so-called core-and-rim structure [25]. A similar reaction can be seen from the microstructure shown in Fig. 16 together with a microprobe scan through the grain. A substantial shift in the [C]/[N] ratio can be observed in the reacted rim, which is caused by the preferential dissolution of "TiC" leaving behind a nitrogen-rich carbonitride. The core is unreacted and still has the starting composition. The formation of the rim probably proceeds via a dissolution–reprecipitation cycle, since the rim has a faceted structure. The higher the carbon content in the titanium carbonitride the more intensive is the contact reaction with Ni, as can be seen from Fig. 17.

5. Conclusions

It has been explained that information on a variety of solid-state properties such as phase equilibria, diffusion kinetics, and homogeneity regions of nitride and carbide phases can be obtained from diffusion couple studies, and even temperature and concentration regions of metastable phase transformations can be determined. This is because the diffusion couples often cover the full composition range so that composition-dependent effects are spatially resolved. As shown for the Ti–N system, further resolution with respect to the temperature axis can be achieved by introducing a temperature gradient so that the two-dimensional imaging of phase reactions is possible.

Further investigations must be made in order to determine concentration-dependent diffusivities, since any f.c.c. monocarbide and mononitride phase shows a large vacancy concentration. In addition, the temperature-gradient diffusion couple technique may be suited to several other systems where the phase diagrams show questionable invariant reactions (compare [8]).

Acknowledgements

The author expresses his gratitude to Prof. Peter Ettmayer for numerous discussions and continued

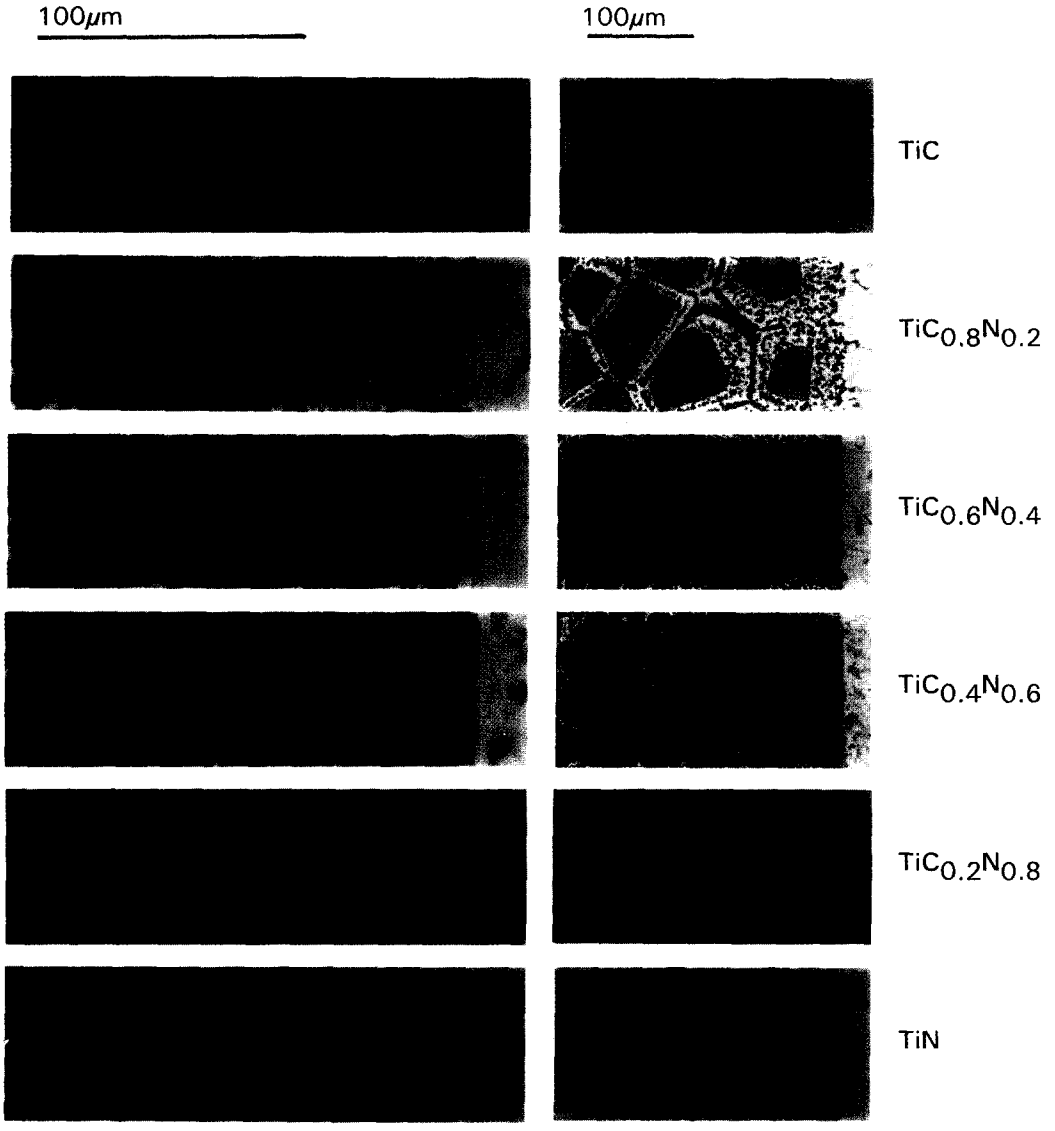

Fig. 17. Contact reaction couples of the series TiCN–Ni reacted for 20 min at 1500 °C [27]. The higher the carbon content, the greater the amount of reaction.

support. Thanks are due to Dr. D. Rafaja and Dipl. Ing. H. Wiesenberger for providing yet unpublished results and to Dr. J. Bauer and M. Bohn for the help with the experimental investigations. Dipl. Ing. C. Jelinek helped with the preparation of the manuscript. Part of this work was supported through projects of the Austrian National Science Foundation, FWF (P7370 and P8487) and of the Oesterreichische Nationalbank (3729).

References

[1] F.J.J. van Loo, *Progr. Solid State Chem.*, *20* (1990) 47.
[2] G.F. Bastin and H.J.M. Heijligers, *Quantitative Electron Probe Microanalysis of Boron in Binary Borides; Quantitative Electron Probe Microanalysis of Carbon in Binary Carbides; Quantitative Electron Probe Microanalysis of Nitrogen*, Eindhoven University of Technology, 1990.
[3] A.D. Romig, Jr., *Bull. Alloy Phase Diagr.*, *8* (1987) 308.
[4] J.L. Pouchou and F. Pichoir, *J. Microsc. Spectrosc. Electron. 10* (1985) 270.
[5] W. Lengauer, J. Bauer, A. Guillou, J.-P. Bars, M. Bohn, E. Etchessahar, J. Debuigne and P. Ettmayer, *Mikrochim. Acta I*, *107* (1992) 303–310.
[6] G.F. Bastin, H.J.M. Heijligers and J.F.M. Pinxter, *Microbeam Analysis*, *290* (1988).
[7] H. Wiesenberger, W. Lengauer and P. Ettmayer, in preparation.
[8] T.B. Massalski, (ed.) *Handbook of Binary Alloy Phase Diagrams*, ASM, Materials Park, OH, 1991.
[9] P. Shewmon, *Diffusion in Solids*, 2nd edn., TMS, Warrendale, 1989.
[10] W. Lengauer, *Acta Metall. Mater.*, *39* (1991) 2985–2996.
[11] W. Lengauer and P. Ettmayer, *J. Phase Equilibr.*, *14* (1993) 162–166.

[12] W. Jost, *Diffusion in Solids, Liquids, Gases*, Academic Press, New York, 1952.
[13] N. Kidson, *J. Nucl. Mater.*, *3* (1961) 21.
[14] D. Rafaja, W. Lengauer and P. Ettmayer (1995) to be published.
[15] J. Philibert, *Atom Movements, Diffusion and Mass Transport in Solids*, Les Editions de Physique, Les Ulis, 1991.
[16] J. Crank, *The Mathematics of Diffusion*, 2nd edn., Clarendon, Oxford, 1975.
[17] R.E. Pawel and J.J. Campbell, *J. Electrochem. Soc.*, *127* (1980) 2188.
[18] W. Lengauer, D. Rafaja, G. Zehetner and P. Ettmayer, in preparation.
[19] W. Lengauer, D. Rafaja, R. Täubler, C. Kral and P. Ettmayer, *Acta Metall. Mater.*, *41* (1993) 3505–3514.
[20] D. Rafaja, Computer codes DIFDK, DIFPW and PROFILE, unpublished, 1995.
[21] F.J.J. van Loo, W. Wakelkamp, G.F. Bastin and R. Metselaar, *Solid State Ionics*, *32* (1989) 824.
[22] H. Wiesenberger, D. Rafaja, W. Lengauer and P. Ettmayer, in preparation.
[23] P. Ettmayer and W. Lengauer, in *Encyclopedia of Inorganic Chemistry*, Wiley, New York, 1994, pp. 2498–2514.
[24] G.F. Bastin, J.H. Maas, F.J.J. van Loo and R. Metselaar, in H. Bildstein and H.M. Ortner (eds.), *Proc. 11th Plansee Seminar*, (1985), Vol. 1, p. 513.
[25] P. Ettmayer, *Ann. Rev. Mater. Sci.*, *19* (1989) 145.
[26] P. Ettmayer, H. Kolaska, W. Lengauer and H. Dreyer, *J. Refract. Hard. Met.*, in press.
[27] S. Binder, W. Lengauer and P. Ettmayer, in F.H. Froes and I.L. Caplan, (eds.) *Titanium '92, Science and Technology*, TMS, Warrendale, PA, 1993, Vol. I, pp. 689–696.